AGU PUBLICATIONS

Geophysical Research Letters

RESEARCH LETTER
10.1002/2015GL065165

Key Points:
- Earthquakes associated with Japan's Ontake eruptions in 2007 and 2014 are detected
- Intense seismicity (dominated by VT earthquakes) indicates the rewaking of Ontake volcano
- LP and LP-associated events may be used to predict the eventual eruption and its eruption location

Supporting Information:
- Supporting Information S1

Correspondence to:
M. Zhang,
zhmiao@mail.ustc.edu.cn

Citation:
Zhang, M., and L. Wen (2015), Earthquake characteristics before eruptions of Japan's Ontake volcano in 2007 and 2014, *Geophys. Res. Lett.*, *42*, doi:10.1002/2015GL065165.

Received 1 JUL 2015
Accepted 12 AUG 2015
Accepted article online 14 AUG 2015

Earthquake characteristics before eruptions of Japan's Ontake volcano in 2007 and 2014

Miao Zhang[1] and Lianxing Wen[1,2]

[1]Laboratory of Seismology and Physics of Earth's Interior, School of Earth and Space Sciences, University of Science and Technology of China, Hefei, China, [2]Department of Geosciences, State University of New York at Stony Brook, Stony Brook, New York, USA

Abstract We detect earthquakes associated with Japan's Ontake eruptions in 2007 and 2014 using the match-and-locate method. Thirty-seven times more events (4949) than the Japan Meteorological Agency (JMA) catalog (133) and 30 times more events (1880) than the JMA catalog (62) are detected during the eruptions of 2007 and 2014, respectively. The detected earthquakes are further classified into three different types: long-period (LP) events, LP-associated events, and volcano-tectonic (VT) earthquakes. Both LP and LP-associated events are observed in the two eruptions. We suggest that the observed intense seismicity before both eruptions indicates the rewaking of Ontake volcano and might be used to predict its impending eruption in the long term. The temporal persistence and spatial concentration of LP and LP-associated events may be used to predict the eventual eruption and eruption location, and the maximum magnitude of the LP events may be used as an indicator of eruption magnitude.

1. Introduction

A volcanic eruption of Mount Ontake took place on 27 September 2014, at approximately 11:52 A.M. Japanese Standard Time (JST). It resulted in 57 casualties, due to lack of warning from the Japanese governmental agencies. Mount Ontake, located on the Japanese island of Honshu around 100 km northeast of Nagoya and 200 km southwest of Tokyo, is the second highest volcano in Japan (after Mount Fuji) with an elevation of 3067 m above sea level. Phreatic eruptions associated with the explosive steam release of heated ground water have occurred at Mount Ontake since at least 6000 years ago [*Kimura and Yoshida*, 1999]. In modern times, Ontake volcano has erupted in 1979, 1991, 2007, and 2014. None showed signs of rising magma, although for the first two eruptions in 1979 and 1991, there was not enough instrumentation in place to rule out magmatic activity [*Cyranoski*, 2014].

Monitoring the activities of various types of the seismic events provides great insight into various physical processes associated with volcanic activity and is also one of the most effective means to predict its eruption [*Chouet et al.*, 1994; *Lahr et al.*, 1994]. Multiphase (gas, liquid, and solid) and various types of medium (magma, water, and rock) coexist in the interior of volcano, causing a variety of types of earthquakes associated with different physical processes. Volcanic earthquakes can be categorized into several types: volcano-tectonic (VT) earthquakes, long-period (LP) events, very-long-period (VLP) events, hybrid events, and volcanic tremor [*Chouet et al.*, 1994; *Chouet*, 1996; *McNutt*, 2002; *Chouet and Matoza*, 2013]. VT earthquakes have clear and broadband *P* and *S* waves with dominant frequencies usually in the 5–15 Hz band, just like typical small tectonic earthquakes. LP events have emergent *P* waves, but no clear *S* waves, with dominant frequencies between 0.5 and 5 Hz [*Chouet*, 1996]. VLP events are similar to LP events but with longer dominant periods in the 2–100 s range [*Chouet and Matoza*, 2013]. Hybrid events have pronounced high-frequency onsets that show the characteristic of VT earthquakes and a nondispersive harmonic coda wave train that exhibits the characteristic of LP events [*Lahr et al.*, 1994]. Volcanic tremor is a continuous signal with the characteristics of LP events but lasting from minutes to days or even longer [*Chouet*, 1996; *McNutt*, 2002]. These different types of events are thought to be related to two basic physical processes that may be occurring during an eruption. The first physical process involves shear or tensile failure in the rock due to stress change caused by the intrusion and/or withdrawal of the fluid, while the second physical process involves pressure fluctuations or sudden changes caused by unsteady mass transport and/or thermodynamics of the fluid [*Chouet*, 1996]. VT earthquakes are related to the first physical process, while LP events, VLP events, and volcanic tremor are related to the second physical process. Hybrid events may involve both processes. VT seismicity is often the first sign of

renewed volcanic activity, and because it can last from days to months or even years before eruption, it may be used as a long-term indicator to an impending eruption, while LP-like events, related to magma transport and activity within shallow conduit systems, have often been used as useful indicators to assess the actual eruption of a volcano [*Chouet et al*., 1994; *Green and Neuberg*, 2006].

Seismometers were first deployed around Ontake volcano in 1976 [*Nakamichi et al*., 2009], but a dense seismic network only became available sometime before the last two eruptions. In this study, we analyze and compare seismicity and earthquake characteristics before the eruptions of 2007 and 2014 and investigate the possible precursory information for the two eruptions. The comparative study of these two eruptions, which occurred at the same location but with different magnitudes, also offers an opportunity to further confirm and elaborate the identified possible precursory information. Although the Japan Meteorological Agency (JMA) reported many earthquakes before both eruptions, more are missing from its catalog. We search for the earthquakes associated with eruptions of 2007 and 2014 using seismic stations within 20 km of eruptions, and a newly developed event detection method called the match-and-locate (M&L) method [*Zhang and Wen*, 2015a]. We also identify LP and their related events in the detected event database and study their possible associations with the eventual eruptions in both time periods.

2. Seismicity Associated With the Eruptions of 2007 and 2014

Although both the 2007 and 2014 eruptions are phreatic, their magnitudes differ significantly. Before the eruption of 2007, intense seismic activity started beneath the summit of Mount Ontake at the end of December 2006 [*Nakamichi et al*., 2009]. A small eruption occurred in late March 2007 (between 16 and 30 March 2007), evidenced by ashfall deposits in the fumarole region south of the summit [*Nakamichi et al*., 2009], although the exact eruption time is unknown due to the absence of visual reports. The eruption of 2014 occurred at 11:52 JST, 27 September 2014, and produced one million tons of ash (http://www3.nhk.or.jp/nhkworld/english/news/mountontakevolcano/20141027.html, last accessed June 2015). Increased seismic activity was also observed in early September 2014 [*Cyranoski*, 2014], approximately 3 weeks before the 27 September eruption. Several craters are involved in the 2014 eruption, with the main crater located at (35.8854°N, 137.4751°E), approximately 1 km southwest of the summit and consistent with the pressure centroids inferred from the observed tilt changes in both the 2007 and 2014 eruptions (Japan Meteorological Agency (JMA), 2014, http://www.data.jma.go.jp/svd/vois/data/tokyo/STOCK/kaisetsu/CCPVE/shiryo/130/130_no01.pdf, last accessed June 2015).

We use the M&L method [*Zhang and Wen*, 2015a] to detect potential earthquakes associated with both eruptions in 2007 and 2014. The M&L method employs some template events and detects small events through stacking cross correlograms between waveforms of the template events and potential small event signals in the continuous waveforms over multiple stations and data components. Unlike the traditional matched filter method which assumes that the template event and slave event are colocated, the M&L method scans over potential small event locations around the template, by making relative traveltime corrections based on the relative locations of the template event and the potential small event before stacking [*Zhang and Wen*, 2015a, 2015b]. The M&L method allows the detection of events with a large distance separation from the template. Furthermore, the locations of detected events can be determined with high precision when good station coverage is available.

Nine three-component seismic stations are located within 20 km of Mount Ontake. Four stations belong to National Research Institute for Earth Science and Disaster Prevention (NIED) (Hi-net and V-net), and five stations belong to Nagoya University. Based on the availability of the seismic data to the public online (http://www.hinet.bosai.go.jp/, last accessed June 2015), we select six stations to study the seismicity associated with the eruptions in 2007 and 2014 (Figure 1a). Among the selected stations, station NU.NGR1 (or NU.NGR) had a name change and was moved a few dozen meters between the two eruptive periods. Such small difference in position should not bias event detections in different time periods.

The seismicity near Mount Ontake based on the JMA catalog shows that earthquakes associated with eruptions occurred within a 4 km × 5 km square area close to the summit (Figure 1a). We collect the data for all the earthquakes in the region listed in the JMA catalog between 1 April 2004 and 25 October 2014 and use these earthquakes as templates in our search through the continuous data for potential earthquakes associated with the eruptions in 2007 and 2014. We select 206 templates after eye-checking the quality of the seismograms recorded by all 18 components (Figure 1b). Due to the lack of station close to the summit of Mount Ontake and imperfect station coverage, earthquake depths cannot be accurately constrained by the M&L

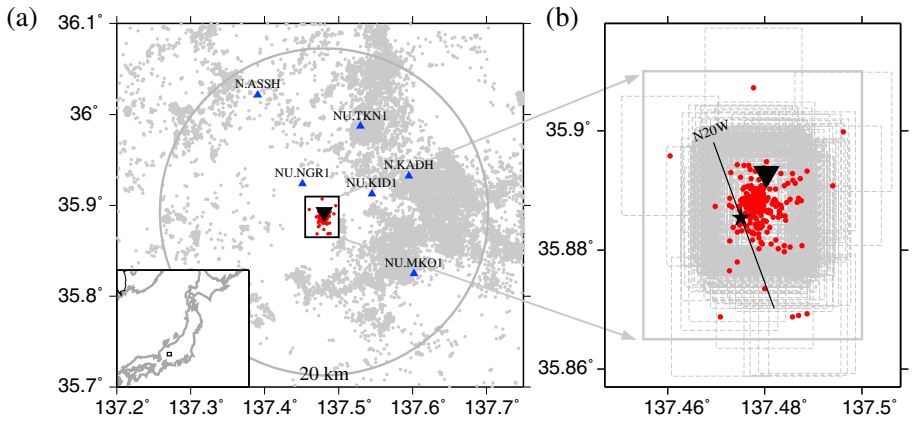

Figure 1. (a) Map showing location of the summit of Mount Ontake (black inverted triangle), historical earthquakes associated with the activity of Ontake volcano (red dots in black rectangle), background seismicity in the surrounding region (grey dots), and six seismic stations (blue triangles) within 20 km of Mount Ontake that are used in the M&L detection of earthquakes. The box indicates the area in Figure 1b. (inset) A regional map of Japan, with the black rectangle indicating the study region. (b) Two hundred six historical earthquakes (red dots within grey rectangle) selected as templates; these events occurred within the black square in Figure 1a. The searched area is a region of 0.02° × 0.02° (grey dashed rectangles) centered at each template location in the M&L method. The main crater and approximate alignment of eruption craters in the 2014 eruption are denoted by a star and a thick black straight line, respectively (JMA, online report, 2014).

method. Therefore, we fix the source depths to those estimated for the templates and search for potential locations of the detected events in a horizontal plane. We carry out our search within a mesh of 0.02° × 0.02° in longitude and latitude centered at each template location, using a grid size of 0.001° (Figure 1b). All templates and continuous data are resampled from 100 Hz to 50 Hz and band-pass filtered from 2 to 8 Hz. *Sg* phases are used, because these have the largest amplitudes in the data. We use a 1-D JMA2001 velocity model [*Ueno et al*., 2002] to calculate the theoretical traveltime and relocation parameters in the M&L method. We consider 4 s waveform segments (1 s before and 3 s after the predicted arrival time of the *Sg* wave) as the template waveforms. Once an event is detected, its magnitude is computed based on the median value of the amplitude ratios recorded at three components of station NU.KID1 (the nearest station NU.NGR or NU.NGR1 is occasionally affected by high-frequency noise, and the seismic signal recorded at more distant stations is buried in the noise when the magnitude of the detected events is smaller than M −1.0).

Using the defined detection thresholds (see supporting information), we search for potential earthquakes in the continuous data from 22 November 2006 to 31 March 2007 and from 1 August 2014 to 25 October 2014, which correspond to the time windows of seismicity associated with the eruptions in 2007 and 2014, respectively.

We detect 4949 earthquakes associated with the eruption of 2007, 37 times more than the total (133) in the JMA catalog in the same time window (Figure 2a). Seismicity started to be active on 18 December 2006. The seismicity fluctuated until mid-January 2007, reached a peak of 350–620 events/day between 16 and 19 January, then decreased quickly and stabilized at 0–20 events/day after 26 January (Figure 2a). A marginal increase in seismic activity occurred in the middle of March 2007, which may be related to the eruption of 2007 (based on the time window of the 2007 eruption suggested by JMA).

We detect 1880 earthquakes associated with the eruption of 2014, 30 times more than the JMA catalog in the same time window (62) (Figure 2b). Seismicity started with 12 events occurring on 31 August 2014 and then decreased gradually with time. Seismicity started to increase gradually from 6 September 2014 to 15 September 2014, with a burst of events on 10 September (158) and 11 September (180). Afterward, the seismicity fluctuated with an average of 30 events/day but showed a clear decreasing trend from 16 September 2014 to 26 September 2014 (Figure 2b). During 7 min before the eruption, intense seismicity (with 29 events) occurred (Figure S1 in the supporting information). After the eruption, the number of events decreased quickly in the following several days.

The earthquakes span a similar geographic region in the 2007 and 2014 eruptions and are mainly concentrated in an area south of the summit (Figure S2 in the supporting information), close to the main crater of the 2014 eruption and near the pressure centroids associated with both the 2007 and 2014 eruptions (JMA, online report, 2014) (Figure 1b).

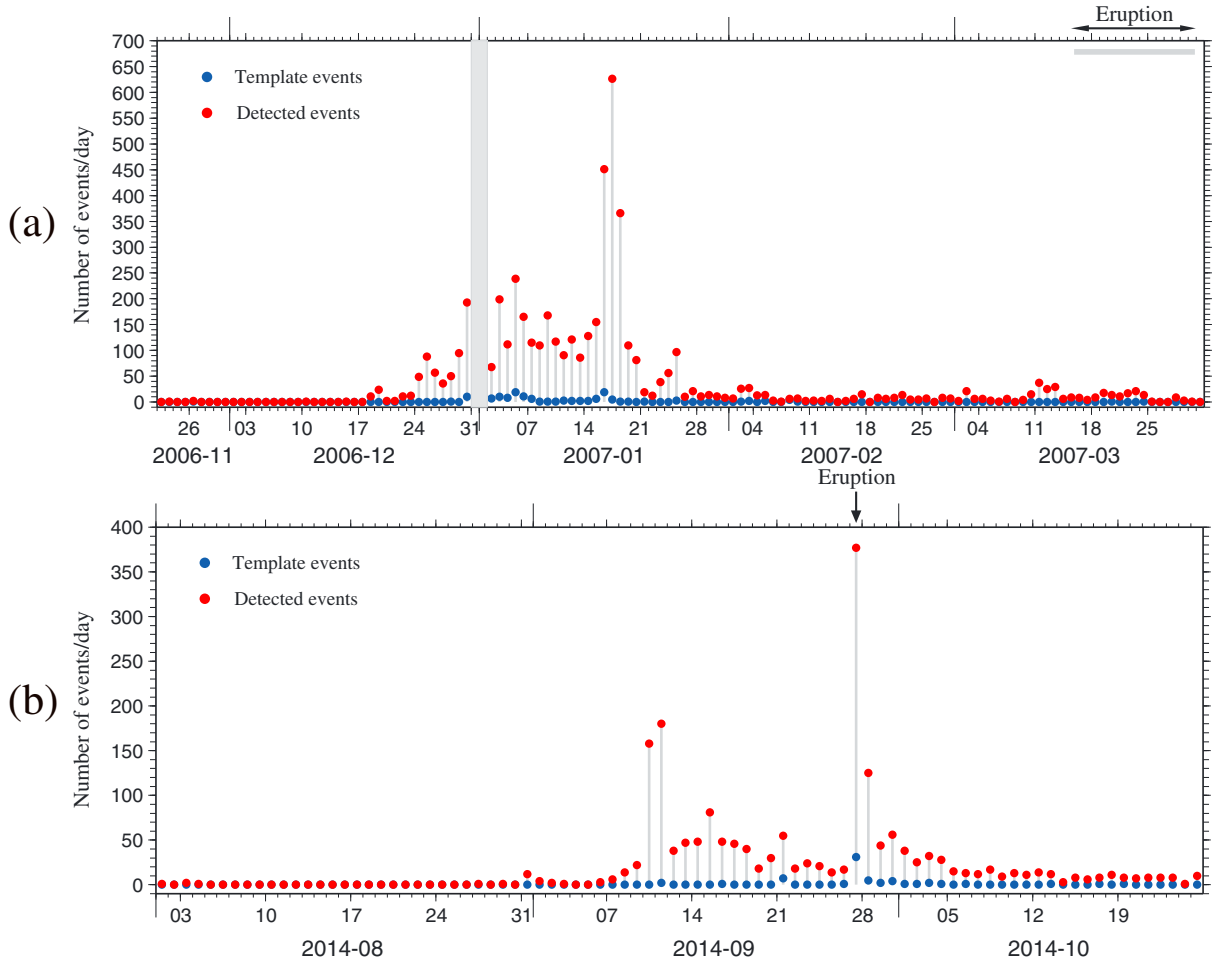

Figure 2. Daily rate of earthquakes detected by the M&L method (red dots) and template events (blue dots) associated with the eruptions of (a) 2007 and (b) 2014. The 2007 eruption is estimated to have occurred between 16 and 30 March 2007 (arrow range in Figure 2a), and the eruption of 2014 occurred at 11:52 JST, 27 September 2014 (vertical arrow in Figure 2b). Grey area indicates the time window of data gap (from 31 December 2006 to 1 January 2007). The smallest magnitude of all the detected earthquakes is M −2.1.

3. Long-Period (LP) and LP-Associated Event Activities During the Two Eruptions

Based on the inspection of event spectra, the detected earthquakes associated with the eruptions in 2007 and 2014 can be classified into three different types: LP events, LP-associated events, and VT earthquakes. LP events exhibit a narrow energy band in the low-frequency range of 1–5 Hz (Figure 3a). LP-associated events are defined here as those that have strong waveform correlation with the classified LP events, including small LP events with low SNR and hybrid events. Other events have spectral characteristics similar to that of VT earthquakes and are classified as VT earthquakes (Figure 3b). As LP and LP-associated events may be directly or indirectly related to the magma process in the region, we identify these events from the earthquake database and study the relationship of their temporal and spatial distributions.

We only carry out the classification for detected events with mean correlation-coefficient (CC) larger than 8.5 times of the right background mean CC (0.041) (i.e., 0.349, the determination of right background mean CC is shown in the supporting information), because they possess higher SNR, and their locations and spectral analysis are reliable. Because the seismic signals of small events are affected by background noise under 1 Hz, we band-pass filter seismic data from 1 to 15 Hz before conversion to frequency domain. LP events are identified using the three-component data at station NU.KID1 (because of its close range and high SNR), and this identification is further confirmed with seismic data from other stations. We use the following criteria: (1) the maximum or average amplitude value of the event spectrum energy in the 1–5 Hz band is 1.2

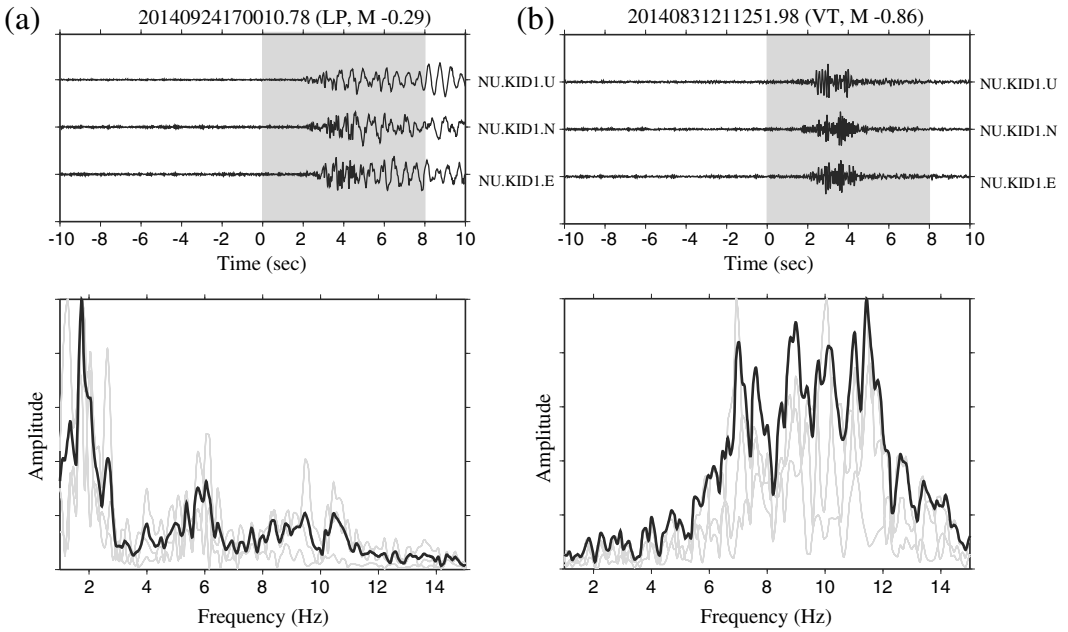

Figure 3. Examples of normalized three-component seismograms and spectra of a (a) LP event and a (b) VT event recorded at station NU.KID1. The spectra (black traces) are the average of the spectra of the three components of seismic data (grey traces), computed in the time windows indicated by the grey rectangles in the top panels. Each subfigure is labeled with event origin time (event type and magnitude). Seismograms are band-pass filtered in a frequency range of 1–15 Hz.

times larger than that in the 5–15 Hz band, (2) event spectrum displays a strong single peak in the dominant frequencies within the 1–5 Hz band, and (3) spectral signature of the seismic data is consistent at all stations. LP-associated events are classified by searching through the continuous seismic record, using the identified LP events as templates and applying the M&L method.

Both LP and LP-associated events are observed in the two eruptions. During the volcanic activity of 2007, we observe 10 clear and reliable LP events with the largest magnitude of −0.73. Seven of these occurred on 2 March 2007. A total of 264 LP-associated events are detected (Figure 4a). In the 2014 eruption, 3 clear and reliable LP events are observed with the largest magnitude of −0.29, and 61 LP-associated events are detected (Figure 4b).

4. Possible Implications of Seismic Activities to Volcano Eruptions

We project all the classified events along the azimuth N20W representing the approximate alignment of eruption craters in 2014 (JMA, online report, 2014) (Figure 1b). The main crater in the 2014 eruption is used as the reference point for the projection (i.e., 0 km in the vertical axes in Figure 4).

Intense VT earthquake activity occurred before both the eruptions of 2007 and 2014. VT seismicity patterns are fairly different between the two eruptions. In 2007, the VT seismicity precedes the eruption by several months and becomes quiescent right before the eruption (Figure 4a); in 2014, VT seismicity occurs within less than one month and grows steadily to maximum before the eruption (Figure 4b). VT seismicity patterns are controlled by the pressure change due to fluid intrusion in the volcano system, background stress field, and closeness to failure of the seismic faults in the region. The observed different patterns of VT seismicity of these two phreatic eruptions that occurred in the same volcano system suggest that VT seismicity response in the volcano region is more a reflection of overall pressure perturbation in the region (or rewaking of the volcano) than an indicator of actual eruption. We suggest that the seismicity (dominated by VT earthquakes) indicates the rewaking of Ontake volcano and might be used to predict its impending eruption in the long term.

The space-time distributions of LP and LP-associated events in the two eruptions exhibit the following characteristics (Figure 4). First, LP and LP-associated events are observed before both eruptions, and their

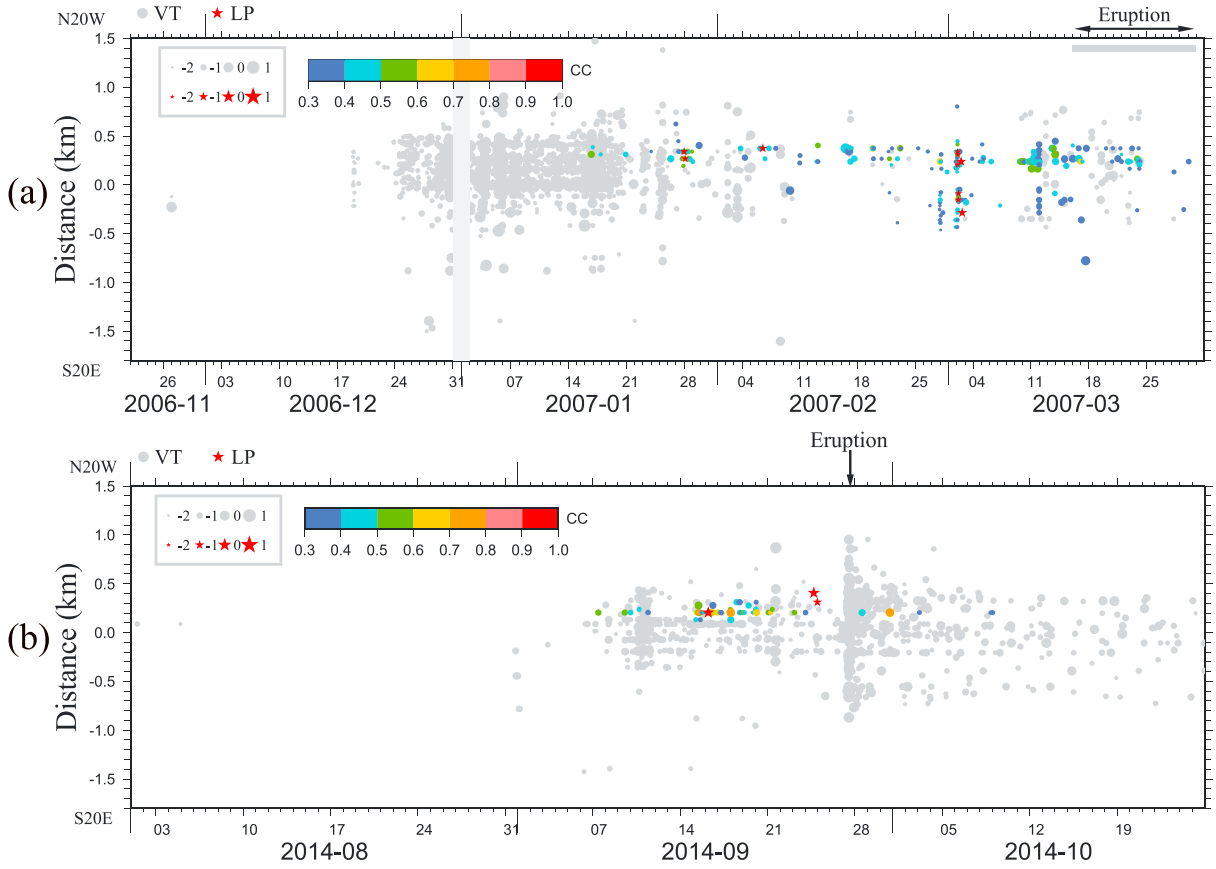

Figure 4. VT earthquakes (grey dots), LP events (red stars), and LP-associated events (colored dots) associated with the eruptions of (a) 2007 and (b) 2014, projected along N20W (Figure 1b). All events are scaled to magnitude, and LP-associated events are color coded by the CC values with their templates. Only events with mean CC larger than 8.5 times of right background mean CC (0.041) (i.e., 0.349) in Figure 2 are shown (the determination of right background mean CC is shown in the supporting information). Eruption times are labeled in the same way as in Figure 2.

locations are close to the pressure centroids imaged for the two eruptions and near the main crater in the 2014 eruption. Although, on some particular days (e.g., 2 March 2007), LP and LP-associated events have scattered locations, the persistent, and most spatially concentrated events are located close to both pressure centroids and main crater of the 2014 eruption (Figure 4). Second, the maximum magnitude of LP events that occurred in 2014 (M −0.29) is larger than the maximum magnitude of LP events in 2007 (M −0.73). We suggest that the LP events are caused by the resonant excitation in a water-filled conduit and reflect mass transport and/or thermodynamics of water, and LP-associated events reflect the effects of pressure transients in the water source. We suggest that the temporal persistence and spatial concentration of LP and LP-associated events may be related to, and may be used as an indicator of, the eventual eruption and eruption location. The properties of LP events (dominant frequency, duration, and amplitude) depend on the geometry of a fluid-filled crack, physical properties of the fluid and solid, and magnitude of pressure transient [*Chouet et al.*, 1994; *Chouet*, 1996]. In the fluid-filled crack model, in particular, the resonant frequency (i.e., dominant frequency) is determined by crack stiffness defined by the bulk modulus of the fluid, the length and aperture of the crack, and the rigidity of the solid; the duration is further controlled by the compressional velocity of the solid, the acoustic velocity of the fluid, and the densities of the solid and fluid; and the seismic amplitude depends on crack properties and magnitude of pressure drop [*Chouet et al.*, 1994; *Chouet*, 1996]. The two largest LP events preceding the two eruptions (20070302153621 and 20140924170010) exhibit similar duration (15 s) and dominant frequency (1.8 Hz), suggesting that they occurred in crack or conduit systems with same or similar properties. Their seismic magnitudes (or the largest amplitudes of the seismic data, which the magnitude determination is based on) should thus directly be related to the pressure drops of the system, and therefore the magnitudes of the eruptions in 2007 and 2014. Given the above physical consideration and the correspondence between the largest

magnitude of LP events and the magnitude of eruption observed between 2007 and 2014, we further propose that the maximum magnitude of the LP events might be related to, and may be used as an indicator of, the eruption magnitude at Ontake volcano.

5. Conclusion

We detect earthquakes associated with Japan's Ontake volcano eruptions in 2007 and 2014, using seismic data recorded at stations within 20 km of the eruptions. The earthquakes are detected with the match-and-locate (M&L) method and are further classified into three different event types based on their spectrum characteristics: long-period (LP) events, LP-associated events, and volcano-tectonic (VT) earthquakes. LP events exhibit a narrow energy band in the low-frequency range of 1–5 Hz; LP-associated events are defined here as those that have strong waveform correlation with the classified LP events (including small LP events with low SNR and hybrid events); and VT earthquakes have spectral characteristics similar to those of small tectonic earthquakes.

We detect 37 times more events (4949) than the JMA catalog (133) in 2007 and 30 times more events (1880) than the JMA catalog (62) in 2014, respectively. Intense seismic activities are associated with both eruptions, consistent with the pressure centroids in the two eruptions and the main crater in the 2014 eruption. We observe 10 clear and reliable LP events and 264 LP-associated events during the 2007 eruption and 3 clear and reliable LP events and 61 LP-associated events in 2014. The persistent and most spatially concentrated LP and LP-associated events are located close to both pressure centroids and the main crater in the 2014 eruption. The maximum magnitude of LP events recorded in 2014 (M −0.29) is larger than that of LP events recorded in 2007 (M −0.73), in good correspondence with the respective magnitudes of the two eruptions. We suggest that LP and LP-associated events are caused by resonant excitation in a water-filled conduit and reflect pressure transients associated with mass transport and/or thermodynamics of water. The temporal persistence and spatial concentration of LP and LP-associated events may be used to predict the eruption and the corresponding eruption location of Ontake volcano, and the maximum magnitude of the LP events may be used to predict the eruption magnitude.

Acknowledgments

We thank the National Research Institute for Earth Science and Disaster Prevention (NIED) and Nagoya University for providing their seismic data. This paper benefited significantly from the reviews by Bernard Chouet and Jackie Caplan-Auerbach. This work was supported by the National Natural Science Foundation of China under grant NSFC41130311 and the Chinese Academy of Sciences and State Administration of Foreign Experts Affairs International Partnership Program for Creative Research Teams.

The Editor thanks Bernard Chouet and Jackie Caplan-Auerbach for their assistance in evaluating this paper.

References

Chouet, B. A. (1996), Long-period volcano seismicity: Its source and use in eruption forecasting, *Nature*, *380*(6572), 309–316.

Chouet, B. A., and R. S. Matoza (2013), A multi-decadal view of seismic methods for detecting precursors of magma movement and eruption, *J. Volcanol. Geotherm. Res.*, *252*, 108–175.

Chouet, B. A., R. A. Page, C. D. Stephens, J. C. Lahr, and J. A. Power (1994), Precursory swarms of long-period events at Redoubt Volcano (1989–1990), Alaska: Their origin and use as a forecasting tool, *J. Volcanol. Geotherm. Res.*, *62*(1), 95–135.

Cyranoski, D. (2014), Why Japan missed volcano's warning signs, *Nature News* (29 September 2014). [Available at http://www.nature.com/news/why-japan-missed-volcano-s-warning-signs-1.16022, last accessed June 2015.]

Green, D. N., and J. Neuberg (2006), Waveform classification of volcanic low-frequency earthquake swarms and its implication at Soufrière Hills Volcano, Montserrat, *J. Volcanol. Geotherm. Res.*, *153*(1), 51–63.

Kimura, J.-I., and T. Yoshida (1999), Magma plumbing system beneath Ontake volcano, central Japan, *Isl. Arc*, *8*(1), 1–29.

Lahr, J., B. Chouet, C. Stephens, J. Power, and R. Page (1994), Earthquake classification, location, and error analysis in a volcanic environment: Implications for the magmatic system of the 1989–1990 eruptions at Redoubt Volcano, Alaska, *J. Volcanol. Geotherm. Res.*, *62*(1), 137–151.

McNutt, S. R. (2002), Volcano seismology and monitoring for eruptions, *Int. Geophys. Ser.*, *81*(A), 383–406.

Nakamichi, H., H. Kumagai, M. Nakano, M. Okubo, F. Kimata, Y. Ito, and K. Obara (2009), Source mechanism of a very-long-period event at Mt. Ontake, central Japan: Response of a hydrothermal system to magma intrusion beneath the summit, *J. Volcanol. Geotherm. Res.*, *187*(3), 167–177.

Ueno, H., S. Hatakeyama, T. Aketagawa, J. Funasaki, and N. Hamada (2002), Improvement of hypocenter determination procedures in the Japan Meteorological Agency, *Q. J. Seismol.*, *65*, 123–134.

Zhang, M., and L. Wen (2015a), An effective method for small event detection: Match and locate (M&L), *Geophys. J. Int.*, *200*(3), 1523–1537.

Zhang, M., and L. Wen (2015b), Seismological evidence for a low-yield nuclear test on 12 May 2010 in North Korea, *Seismol. Res. Lett.*, *86*(1), 138–145.